

SUPPLEMENTAL MATERIALS

SUPPLEMENTAL METHODS:

Tissue isolation and single-cell sequencing using the 10x Genomics® platform:

Dissected tissues were then dissociated into single cells in a microcentrifuge tube with 100 µl of 0.25% trypsin and incubating at 37°C for 10 min. Subsequently, 1.4 mL of collagenase A/B (10 mg/mL, Roche) and 20% FBS serum in HBSS was added to the microcentrifuge tubes and tissue samples were returned to 37°C water bath for an additional 20 min. Cells were then spun down at 1000 RPM for 5 min, supernatant was removed and cells were washed in 20% FBS in HBSS. After suspension, cells were resuspended to around 600 cell/µl with 0.04% FBS/HBSS solution for processing on the 10x Platform.

Prepared cells were captured with 10x chromium by following the Chromium™ single-cell 3' reagent kits v2 user guide. Briefly, single cells were partitioned into nanoliter-scale Gel Bead-In-EMulsions (GEMs) in the Chromium™ controller. After dissolution of the Gel beads in GEMs, the primers were released, and mRNA were reverse transcribed into barcoded cDNA library. After further cleanup and amplification, the cDNA was enzymatically fragmented and 3' end fragments were selected for library preparation. After further end repair, A-tailing, adaptor ligation and PCR amplification, sample index, UMI sequences, barcode sequences, and sequencing primer P5 and P7 on both ends were added to cDNA. The libraries were sequenced using Illumina HiSeq 4000.

Bioinformatics:

Seurat determines adjusted p-values based on Bonferroni correction using the total number of genes within each dataset. Therefore, the number of tests corrected for in the Zone I dataset was 17,264, Zone II was 16,855 and Zone III was 27,998.

Immunofluorescence: Immunofluorescence staining was carried out by following previous protocol with minor modifications⁵⁶. Briefly, CD1 mouse embryos from indicated gestational ages were isolated by dissection, washed in HBSS (+Ca/+Mg) (Gibco, 14025-134) prior to fixation overnight in 4% paraformaldehyde (Fisher, 50-980-487) at 4°C. Hearts were then washed in PBS for 15 min three times prior to incubation in 30% sucrose in PBS overnight at 4°C and then embedded in Tissue-Plus OCT (Fisher, 23-730-571). The embryos were cut as cryosections of 12 µm thickness and stored at -80°C. The sections were dried for 1 hour prior to use, rehydrated in PBS, washed three times in PBST (PBS + 0.1% Triton X100) and then blocked (PBST + 0.5% Bovine serum albumin) for 1 hour at room temperature. Following this, the sections were incubated with primary antibodies diluted in blocking solution overnight at 4°C in humid chambers. Primary antibodies used included: Anti-mouse Igfbp5 Goat Polyclonal Antibody (R&D systems/Fisher Scientific: AF578) at 1:100 dilution; Anti-mouse Connexin 40 Rabbit Polyclonal antibody (Alpha Diagnostics, Cx40-A) at 1:100 dilution; Anti-mouse Hcn4 Rat Monoclonal [SHG 1E5] antibody (Abcam, ab32675) at 1:75 dilution.

On the second day, after washing three times with PBST, the sections were incubated with secondary antibody for 2 hours at room temperature. The following secondaries were used at a 1:500 dilution: Donkey anti-goat IgG Alexa Fluor 555 (Invitrogen, A-21432), Chicken anti-Rabbit

IgG Alexa Fluor 488 (Invitrogen, A-21441), Donkey anti-Rabbit IgG Alexa Fluor 647 (Invitrogen, A-31573) and Chicken anti-Rat IgG AlexaFluor 488 (Invitrogen A-21470). After additional washing with PBS for 5 minutes three times, the sections were mounted with mounting media containing DAPI (Vector Laboratories, H-1200). All images were taken with Axioimager microscope at Neuroscience Microscope Service (NMS) facility at Stanford University. Negative controls for immunostaining included the use of primaries or secondary antibodies alone. A minimum of 4 biological (different hearts) and 4 technical (different slides/heart) replicates were used for each antibody staining.

Online Figure Legends:

Online Figure I. GO/KEGG Term Enrichment Analyses of Zone I Non-Cardiomyocyte Lineages.

Pathway enrichment analysis on all non-cardiomyocyte clusters of Zone I. Statistically significant gene ontologies were consistent with suspected cluster identities based on differential gene expression including fibroblasts (Clusters 2, 5, 6, 11), endocardial/endothelial cells (Clusters 4, 7, 13), white blood cells (Cluster 8), epicardial cells (Cluster 10) and neuronal cells (Cluster 14). Dot size is proportional to the number of differentially expression genes within a given pathway; the color is proportional to the significance (FDR adjusted p-value).

Online Figure II. Comparison of SAN Gene Enrichment in Bulk vs. scRNA Sequencing.

(A) Table modified from *Vedantham et al. 2015*²⁰ listing the 30 most significant differentially expressed sinoatrial node (SAN) genes. RNA sequencing data from this prior study was generated from SAN tissue (vs. right atrial (RA) myocardium) isolated by laser capture microdissection on unfixed, unstained cryosections from flash-frozen *Hcn4*-GFP (green-fluorescent protein) transgenic mouse hearts harvested at embryonic day 14.5 (E14.5). Right side of table shows the corresponding cluster enrichment of highlighted genes from the current study's RNA-seq data within Zone I of E16.5 mice. Genes highlighted in green represent known SAN genes. Genes highlighted in red represent examples of enrichment due to suspected contaminant cells as listed. Gm15415 encodes a predicted long non-coding RNA that was not detected within our dataset under its current name. CM, cardiomyocyte. **(B)** Gene expression enrichment across all 15 clusters within Zone I. Cluster 9 (C9) represents the putative SA nodal cluster, while other atrial cardiomyocyte clusters include C0, C1, C3, C12, C15. Additional clusters, based on their respective gene expression profiles, include fibroblasts (Clusters 2, 5, 6, 11), endocardial/endothelial cells (Clusters 4, 7, 13), epicardial cells (Cluster 10), white blood cells (Cluster 8) and neuronal cells (Cluster 14).

Online Figure III. Comparison of SAN Gene Enrichment in *Tbx3*-Sorted vs. scRNA Sequencing.

(A) Table modified from *Van Eif et al. 2019*²¹ listing the reported top 16 differentially expressed sinoatrial node (SAN) genes in sorted *Tbx3*-Venus⁺ cells versus *Kat5*⁺ cells from embryonic day 17.5 (E17.5) mice. Right side of table shows the corresponding cluster enrichment of highlighted genes from the current study's RNA-seq data within Zone I of E16.5 mice. Genes highlighted in green represent known SAN genes. Genes highlighted in red represent examples of enrichment due to suspected contaminant cells as listed. **(B)** Gene expression enrichment across all 15 clusters within Zone I. Cluster 9 (C9) represents the putative SA nodal cluster, while other atrial cardiomyocyte clusters include C0, C1, C3, C12, C15. Additional clusters, based on their respective gene expression profiles, include fibroblasts (Clusters 2, 5, 6, 11), endocardial/endothelial cells (Clusters 4, 7, 13), epicardial cells (Cluster 10), white blood cells (Cluster 8) and neuronal cells (Cluster 14).

Online Figure IV. *Igfbp5* is Expressed Within the Compact SAN and Transitional Cells but Not Within the SAN Artery.

Immunofluorescent staining (n=5) of a postnatal day 12 (P12) wild-type murine cardiac tissue sections showing a compact SAN (cSAN) (outlined by solid line), transitional cells (Tz) (dashed line) populations and SAN artery (SAN Art.) labelled by Cx40 (green). *Igfbp5* (red). RA, right atrial myocardium.

Online Figure V. *Igfbp5*, *Cpne5*, *Smoc2*, *Rgs6* and *Ntm* are Enriched in the Compact SAN and Transitional Cells of the Mouse Heart.

Immunofluorescent staining of wild-type murine cardiac tissue sections showing the compact SAN (cSAN) (outlined by solid line) and transitional cell (Tz) (dashed line) populations. (A) *Igfbp5* (red), Cx40 (green) and *Hcn4* (blue); E14.5 heart (n=5). (B) *Cpne5* (red) and *Hcn4* (blue); E16.5 heart. (n=6) (C) *Smoc2* (red) and Cx40 (green); P0 heart. (D) *Rgs6* (red) and *Hcn4* (blue); E16.5 heart. (n=6) (E) Fluorescent RNA *in situ* hybridization targeting *Hcn4* (red punctae) and *Ntm* (green punctae) mRNA expression within P0 mouse heart sections (n=3). DAPI (blue). RA, right atrial myocardium; SAN Art., SAN artery.

Online Figure VI. Expression of *Igfbp5*, *Cpne5*, *Rgs6* and *Ntm* Within cSAN and Transitional Cell Subclusters of Cluster 9. Expression of each gene represented by ViolinPlot (top) and FeaturePlot (bottom) within the compact SAN (cSAN) and transitional cell (Tz) subclusters of Cluster 9 from Zone I.

Online Figure VII. Analysis of *Hcn4*⁺ Cells in Zone I Reveal Compact SAN Subtypes Consistent with Head and Tail Regions. (A) Diagram detailing workflow and cell numbers for *Hcn4* positive and negative cardiomyocytes (CM) isolated for further analysis from the total number of cells within Zone I. (B) t-SNE plot of 127 *Hcn4*⁺ cardiomyocytes (*Hcn4*⁺/*Actn2*⁺) revealed two distinct cell subpopulations consistent with SA nodal “Head” and “Tail” cells. (C) General CM signature (*Tnni3*⁺) demonstrating that both clusters are indeed CMs. (D) Illustration of known functional SAN subdomains including the “Head” (*Hcn4*^{hi}/*Shox2*⁺/*Tbx18*⁺/*Nkx2-5*⁻) and “Tail” (*Hcn4*^{low}/*Shox2*⁺/*Tbx18*⁻/*Nkx2-5*⁺) cells with representative enriched (green) and repressed (red) genes. (E) Gene signature of SAN Head vs Tail gene expression visualized by ViolinPlots (left) and FeaturePlots (right).

Online Figure VIII. *Igfbp5*, *Rgs6* and *Ntm* are Enriched in the Murine AVN.

Immunofluorescent staining of wild-type murine cardiac tissue sections showing the AVN. (A) *Igfbp5* (red) and Cx40 (green); P4 heart (n=4). Four panels showing progressively more anterior sections (A.1-A.4). Inset showing an enlarged area of AVN region. Note the AVN (*Igfbp5*⁺/*Cx40*^{neg}) gives rise to the His bundle (*Igfbp5*⁺/*Cx40*⁺) as the sections move anteriorly. Gene expression visualized by ViolinPlots showing enrichment in Cluster 4 (AVN Cluster). White arrow, AVN; purple arrow, His bundle; red arrows, internodal tracks; blue arrows, right AV ring bundle; yellow arrows, left AV ring bundle. (B) *Rgs6* (white) with inset showing AVN; E16.5 heart (n=6). Gene expression visualized by ViolinPlots showing enrichment in Cluster 4 (AVN Cluster). (C) DAPI stain (white) of a P0, wild-type heart with the AVN and surrounding cardiac structures labelled. LA, left atrium; LV, left ventricle; MV, mitral valve. *Ntm* gene expression visualized by ViolinPlots showing enrichment in Cluster 4 (AVN Cluster). (D) Magnification of the boxed AVN region in subpanel C with fluorescent RNA *in situ*

hybridization targeting *Hcn4* (red punctae) and *Ntm* (teal punctae) mRNA; DAPI in blue. (n=3) AVN, surrounding internodal tracks (INT) (above) and ventricular cardiomyocytes (below) of the interventricular septum (IVS) are labeled. Solid lines demarcating the AVN. Larger brightly-stained objects (examples noted by white arrows) in both red and green channels represent autofluorescence from red blood cells (yellow in merge photos). True fluorescent *in situ* hybridization signal is represented by small punctae in either green (*Ntm*) or red (*Hcn4*).

Online Figure IX. *Cpne5* Expression in Cluster 4 Cell Subtypes.

Cpne5 expression represented by ViolinPlot (left) and FeaturePlot (right).

Online Figure X. *Igfbp5* and *Cpne5* Are Expressed in the Ventricular Conduction System.

(A) Anti-Igfbp5 immunofluorescence stain (white) within E16.5, wild-type mouse heart. (n=8) All ventricular conduction system components labelled. (B) Fluorescent RNA *in situ* hybridization (n=3) demonstrating overlap of *Hcn4* (red punctae) and *Cpne5* (green punctae) expression within the Purkinje fibers of a P0 wild-type mouse heart. DAPI (blue). Solid line depicting standard immature PF cells (*Hcn4*⁺/*Cpne5*⁺) and dashed line showing Tz cells (*Hcn4*^{low/neg}/*Cpne5*⁺). Beyond these borders are ventricular myocardial (VM) cells (*Hcn4*^{neg}/*Cpne5*^{neg}). His, His bundle; LBB, left bundle branch; PF, Purkinje fiber; RBB, right bundle branch; Tz, Transitional cells.

Online Figure XI. *Igfbp5* is Enriched Within the Entire Cardiac Conduction System.

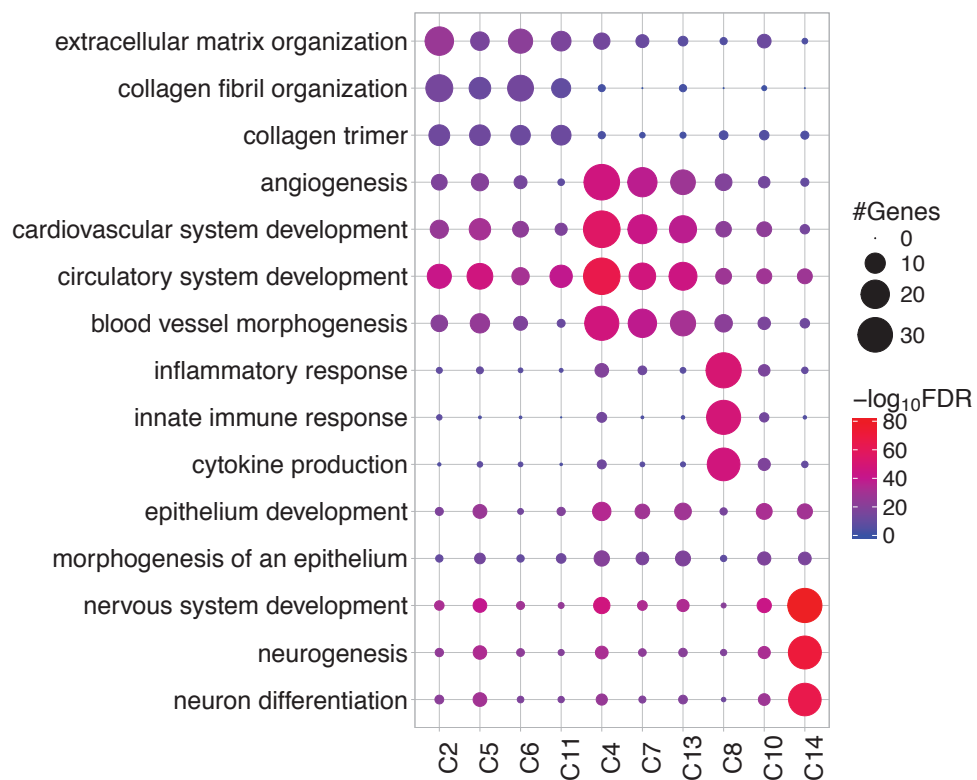
(A) Fold enrichment of *Igfbp5* expression within Cluster 9 in Zone I (“SAN” Cluster), Cluster 4 in Zone II (“AVN/His” Cluster) and Cluster 13 in Zone III (“PF” Cluster) as compared to all other cells within each respective zone. (B) E16.5 wild-type mouse heart (above) with corresponding two-dimensional z-projections (below) from indicated z-planes. *Igfbp5* expression shown in white with conduction system components labelled. (n=10) (C) iDISCO+ with immunostaining for Cx40/Gja5 (green) and *Igfbp5* (red) protein. Note the reciprocal labelling of SAN tissue (*Igfbp5*, red) versus the surrounding atrial working myocardium (Cx40, green). (n=4) AVN, atrioventricular node. His, His bundle. INT, internodal tracks. LBB/RBB, left of right bundle branch. PF, Purkinje fiber. SAN, sinoatrial node.

Online Figure XII. Optical Clearing and 3D Volumetric Analyses Illustrate Transitional Cell Populations Exiting the SAN. (A) iDISCO+ cleared wild-type SAN (6.3x magnification) co-immunolabeled for *Hcn4* (red) and *Smoc2* (green) protein from a postnatal day 12 (P12) heart. SAN shown at three angles of view (0, 90, ~225 degrees). Merge image (*Hcn4* in red, *Smoc2* in green) with two major transitional sinoatrial conduction pathways (SACPs) outlined (*Hcn4*^{neg}/*Smoc2*⁺). Purple SACP: from SAN body directed rightward; Black SACP: from the SAN head directed inferiorly and leftward. A third *Hcn4*⁺ SACP is also marked by *Smoc2* and emerges inferiorly from the tail of the SAN to give rise to the internodal tracks (blue line), not shown here. (B-C) Immunolabeling of *Igfbp5* (B) and *Cpne5* (C) (both purple) within the SANs of P0 and P12 murine hearts, respectively. Similar SACP pathways are outlined as above.

Online Movie I. *Igfbp5* Delineates the Entire Cardiac Conduction System Within an Optically Cleared, Intact Mouse Heart. Embryonic day 16.5 (E16.5) wild-type, whole heart optically cleared using iDISCO+ technique, labeled with anti-Igfbp5 antibody (red) and visualized with light sheet microscopy. (n=10) 3D image processing using Imaris software. Movie provides 360 degree views in both the vertical and horizontal axes.

Online Movie II. *Cpne5* Delineates the Entire Cardiac Conduction System Within an Optically Cleared, Intact Mouse Heart. Postnatal day 12 (P12) wild-type, whole heart optically cleared using iDISCO+ technique, labeled with anti-Cpne5 antibody (green) and visualized with light sheet microscopy. (n=10) 3D image processing using Imaris software. Movie provides 360 degree views.

Online Movie III. *Rgs6* Marks the Compact SAN and Transitional Cell Populations Within an Optically Cleared, Intact Mouse Heart. iDISCO+ cleared wild-type, intact SAN (6.3x magnification) from E16.5 murine heart co-immunolabeled for Hcn4 (red) and Rgs6 (green) protein (n=8) 3D image processing using Imaris software. Movie provides 360 degree views.

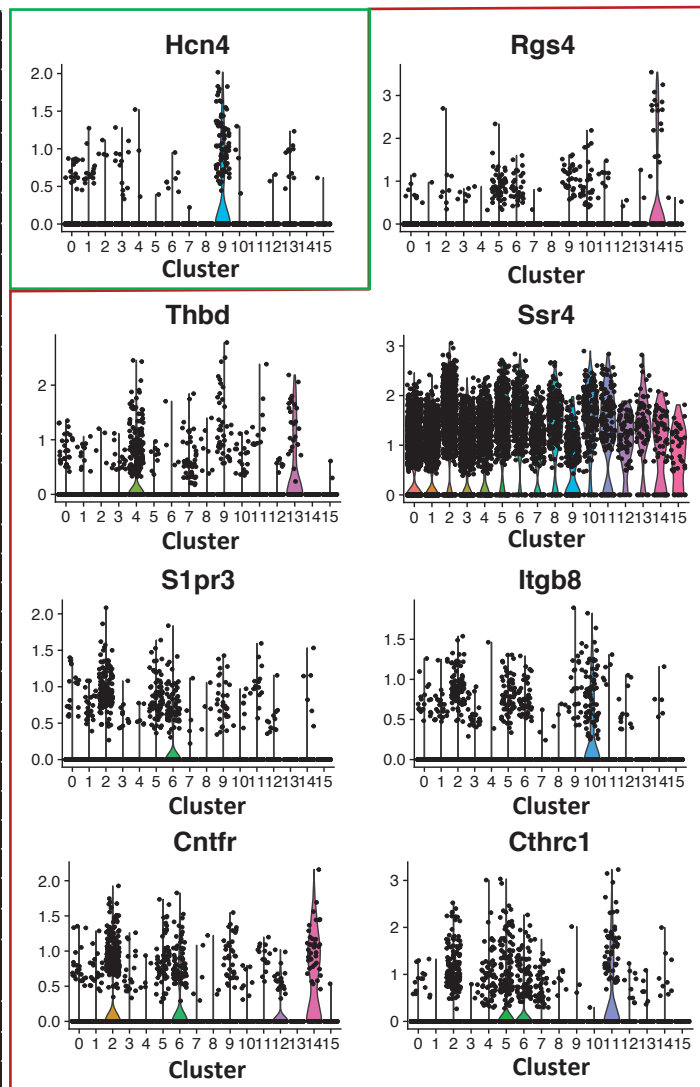


Online Figure I. GO/KEGG Term Enrichment Analyses of Zone I Non-Cardiomyocyte Lineages.

A.

Modified from <i>Vedantham et al. 2015</i>			Current Study	
Gene	Log(2) Fold-Change RA vs SAN	p-value	Cluster Enrichment for Zone I	Associated Cluster Identities
Isl1	-14.28835332	2.81E-75	C9, C14	SAN/Neuronal
Smoc2	-7.383172348	1.62E-69		
Rgs4	-8.598664639	1.60E-57	C14	Neuronal
Hcn4	-5.873773035	1.94E-43	C9	SAN
Tbx3	-7.143232512	1.47E-39	C9, C14	SAN/Neuronal
Shox2	-6.282438792	4.58E-37	C6, C9, C12	SAN/ Fibroblast/CM
Gm15415	-5.106812377	4.52E-37	Not detected	Not detected
Odz4	-4.143877804	1.70E-33		
Csmd1	-6.364072299	1.51E-30		
Vsnl1	-4.37227765	3.80E-28		
Dmrt2	-8.068581086	8.53E-28		
Thbd	-4.645158256	1.09E-27	C4, C13	Endocardial/ Endothelial
Gabra3	-4.819268604	3.17E-27		
Syn2	-5.673823248	4.43E-27		
Gm2301	-11.58561666	4.33E-26		
Kif1a	-4.21900186	7.00E-25		
Cckar	-8.063142611	2.06E-24		
Ssr4	-6.273610875	6.97E-22	All Clusters	N/A
Rgs6	-3.20300397	1.00E-21		
Hcn1	-5.343241944	1.13E-21	C9	SAN
Bmp2	-4.415253764	7.50E-21		
Mfsd6	-2.998749942	8.15E-21		
Gucy2e	-10.86679374	2.45E-20		
Uchl1	-4.439850542	3.19E-20		
S1pr3	-3.188558335	4.40E-20	C6	Fibroblast
Itgb8	-3.177652546	1.34E-19	C10	Epicardial
Cntfr	-4.646736865	1.88E-19	C2, C6, C12, C14	Fibroblast/CM/ Neuronal
Cthrc1	-8.61221459	6.65E-19	C2, C5, C6 C11	Fibroblast
Fzd7	-2.84996998	4.15E-18		
Ramp1	-3.794472111	5.76E-17		

B.

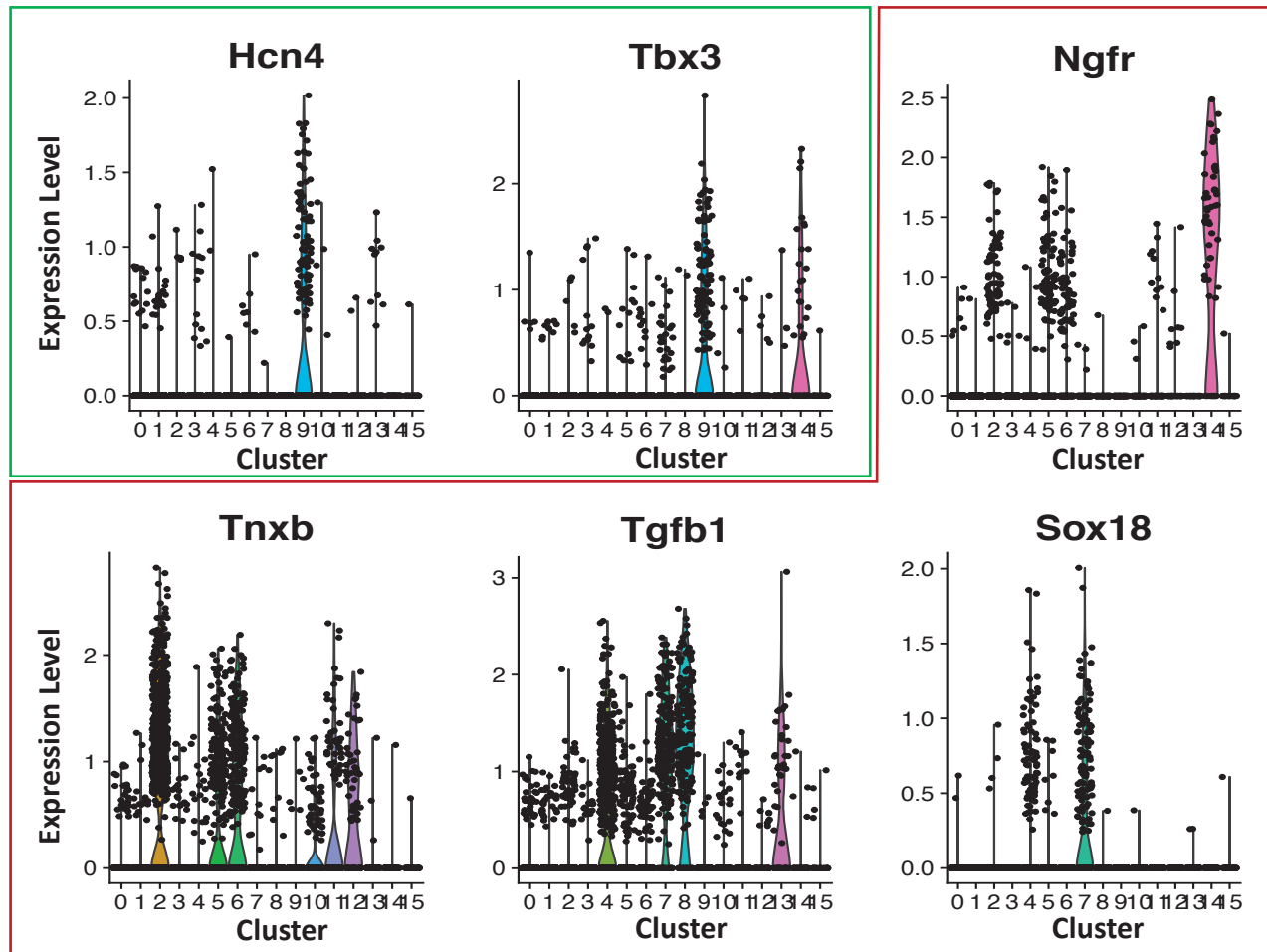


Online Figure II. Comparison of SAN Gene Enrichment in Bulk vs. scRNA Sequencing.

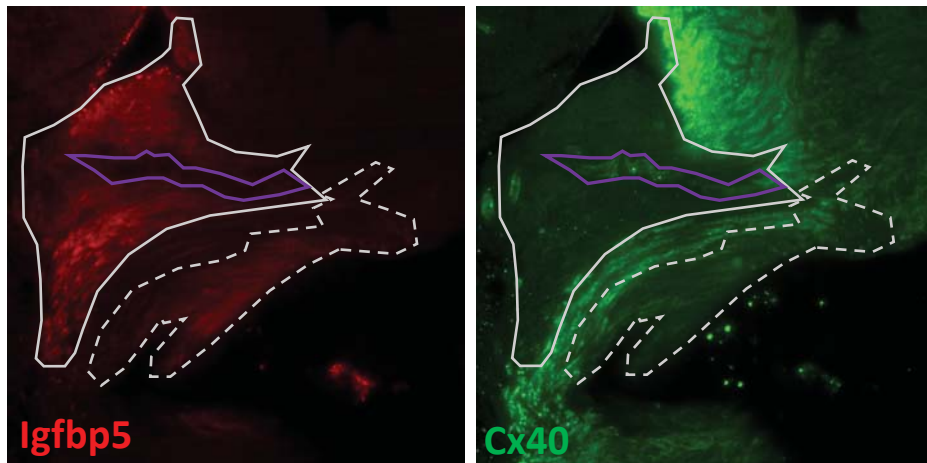
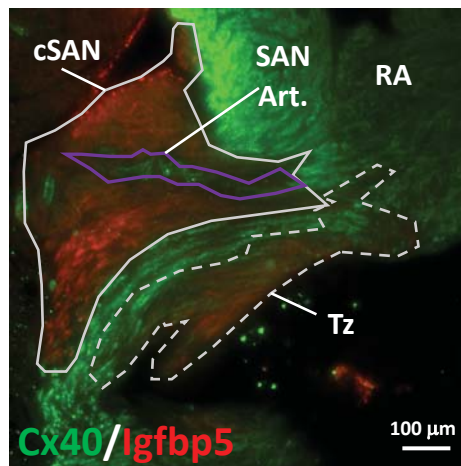
A.

Modified from <i>Van Eif et al. 2019</i>			Current Study	
Gene	Log(2) Fold-Change RA (Katushka+) vs SAN (Venus+)	p-value	Cluster Enrichment for Zone I	Associated Cluster Identities
Ngfr	-6.604350686	2.70E-41	C14	Neuronal
Ntrk3	-6.500756702	1.95E-24	C11	Fibroblast
Figf	-6.453818752	1.03E-12	C2, C6	Fibroblast
Tnxb	-6.44060532	9.43E-18	C2, C5, C6, C10, C11, C12	Fibroblast/Epicardial/CM
Tgfb1	-6.297994994	6.46E-14	C4, C7, C8, C13	Endocardial/WBC/Endothelial
Nfasc	-6.233087993	3.18E-35	C9	SAN
Sox18	-6.228369461	3.41E-12	C4, C7	Endocardial
Ltbp4	-6.102507339	3.04E-21	C2, C4, C5, C6, C7, C10, C11, C12	Fibroblast/Endocardial/Epicardial/CM
Hcn4	-6.044298097	9.64E-19	C9	SAN
Adam12	-5.95992986	1.14E-20	C2, C5, C6	Fibroblast
Shox2	-5.958662083	6.81E-26	C6, C9, C12	SAN/Fibroblast/CM
Col15a1	-5.94994844	5.73E-31	C4, C7, C14	Endocardial/Neuronal
Aatk	-5.897518412	7.85E-18	C14	Neuronal
Fndc1	-5.809981383	5.12E-16	C2, C5, C6, C10, C11, C12	Fibroblast/Epicardial/CM
Ptprz1	-5.789636644	3.88E-17	C14	Neuronal
Tbx3	-5.77333563	3.30E-29	C9, C14	SAN/Neuronal

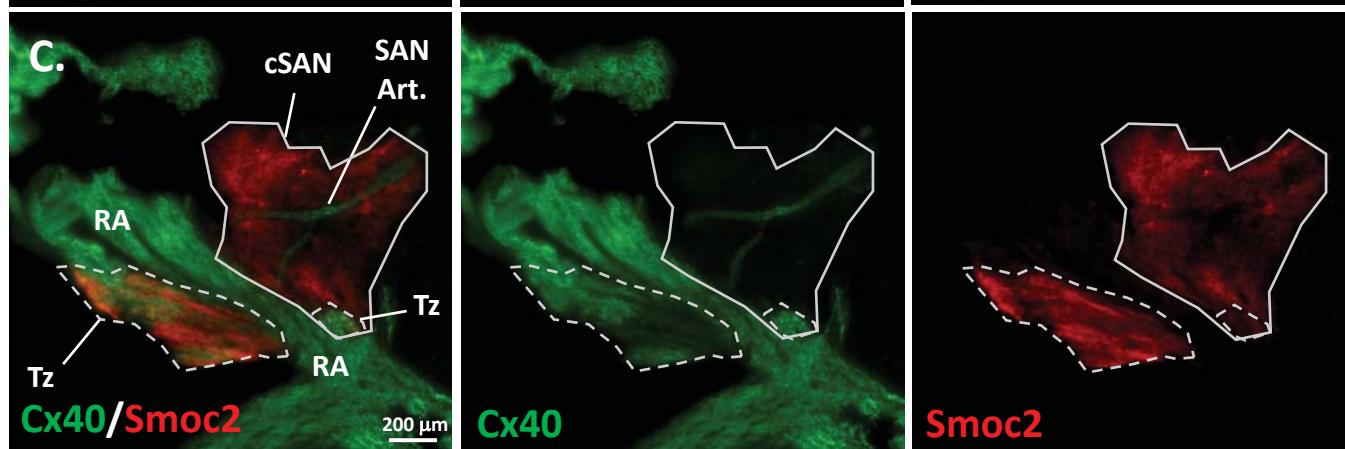
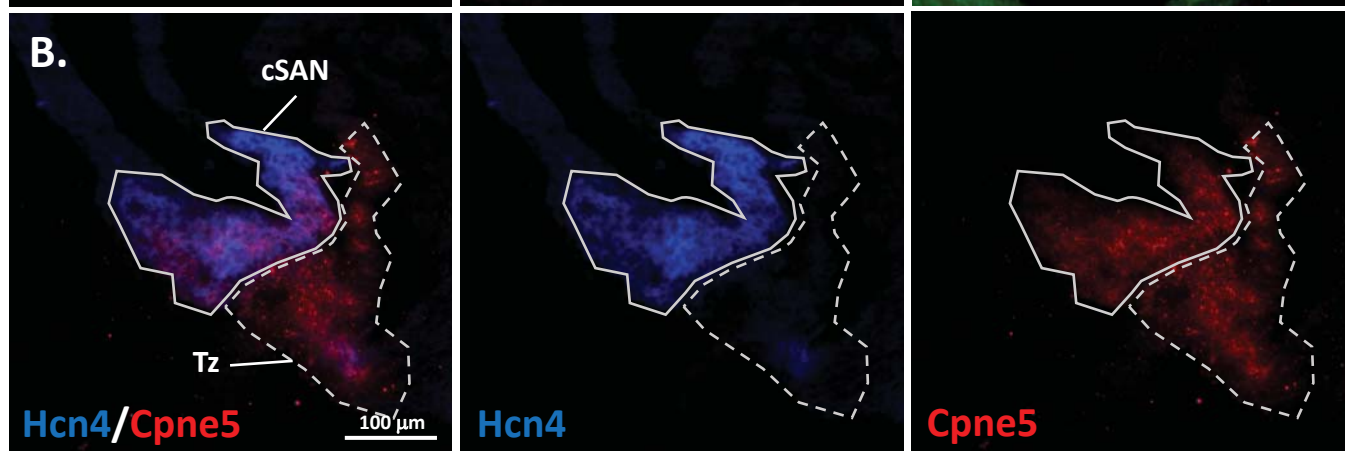
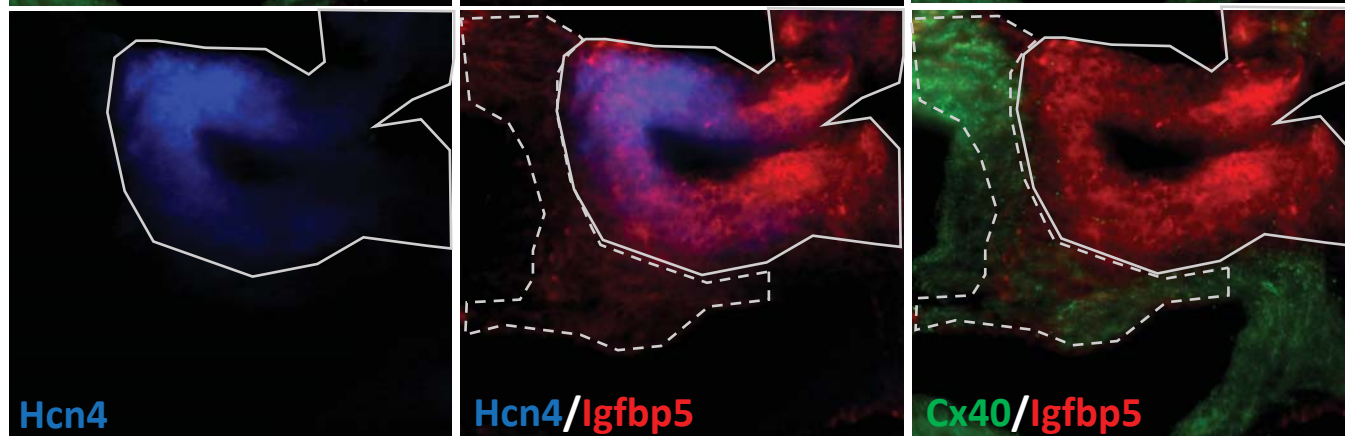
B.

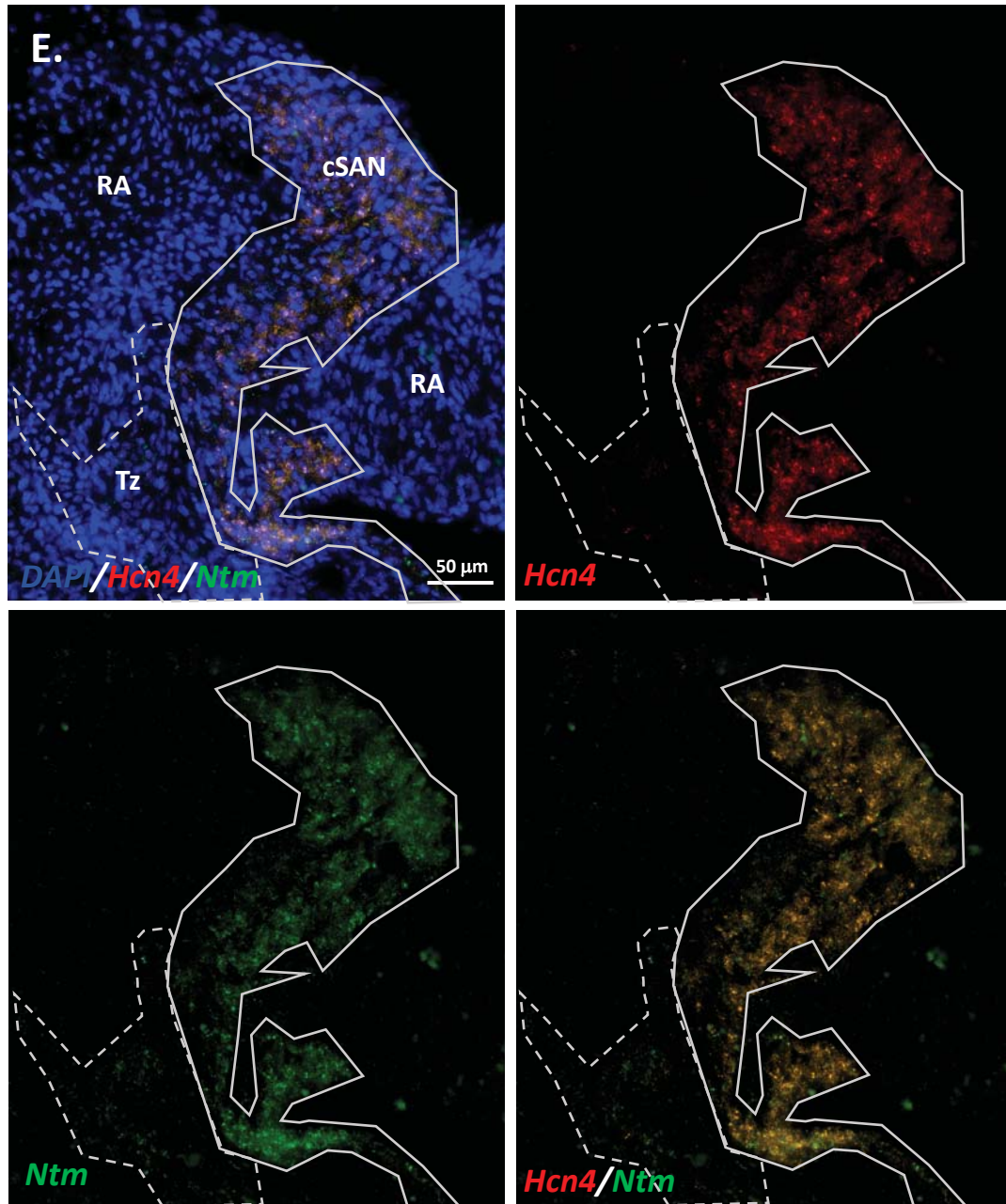


Online Figure III. Comparison of SAN Gene Enrichment in Tbx3-sorted vs. scRNA Sequencing.

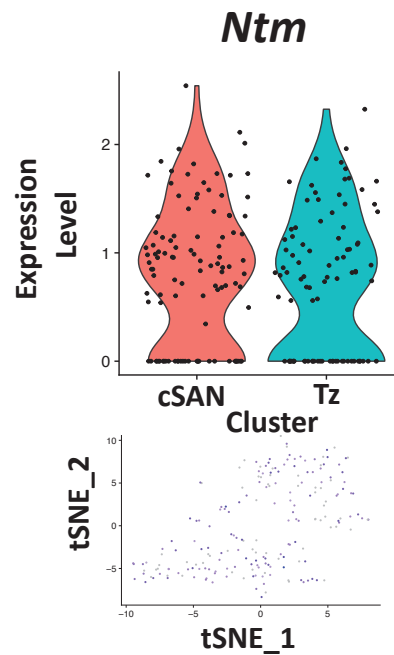
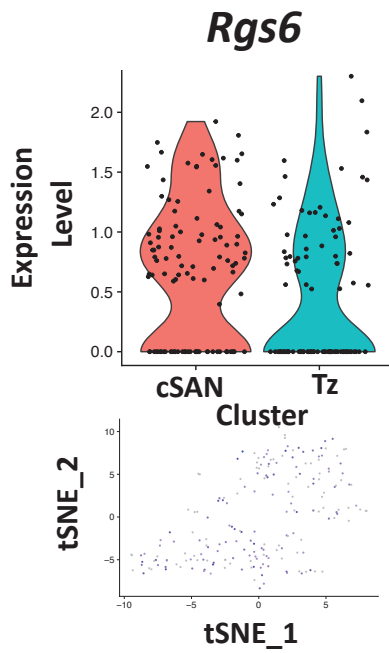
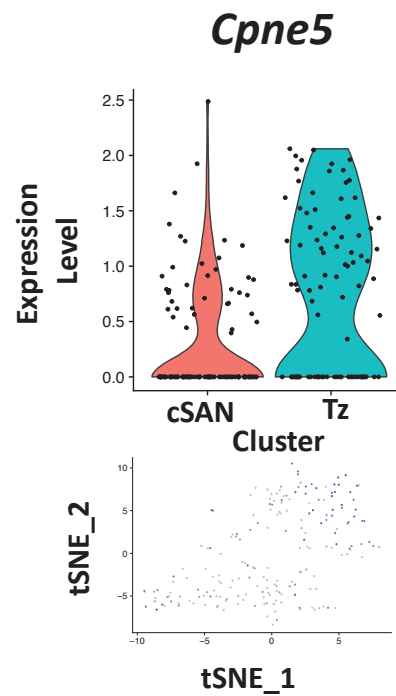
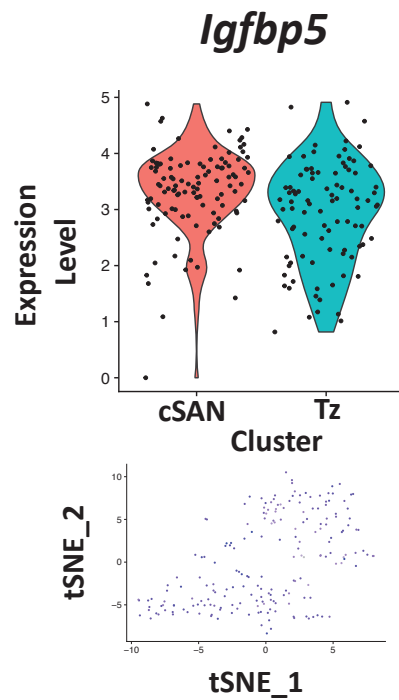


Online Figure IV. *Igfbp5* is Expressed Within the Compact SAN and Transitional Cells but Not Within the SAN Artery.

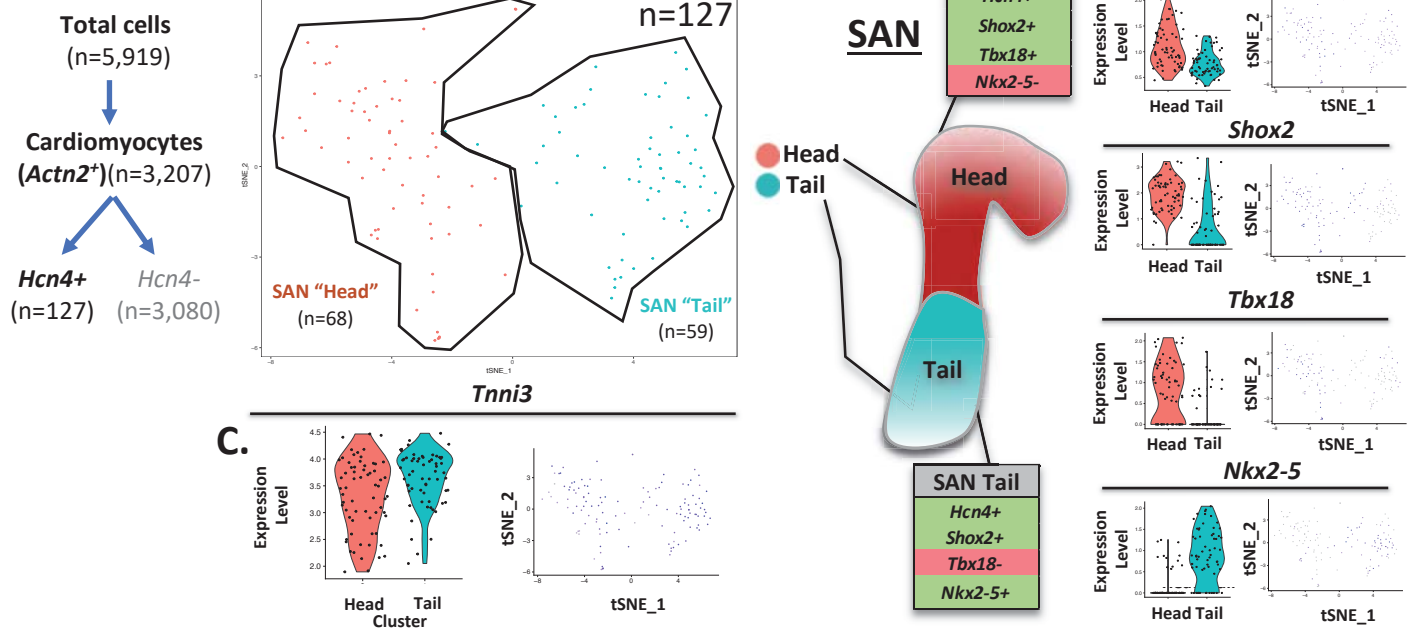




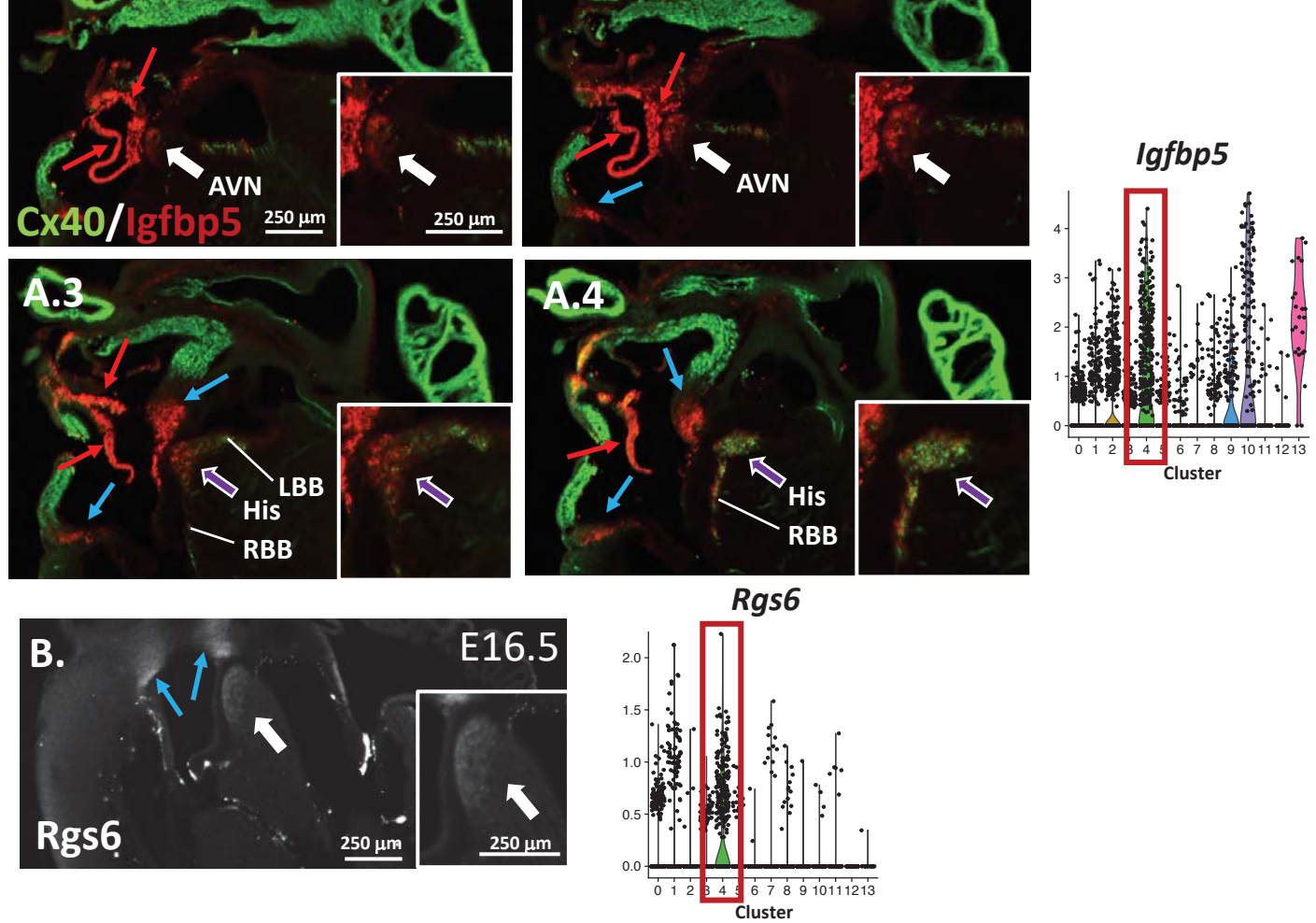
Online Figure V...continued. *Igfbp5*, *Cpne5*, *Smoc2*, *Rgs6* and *Ntm* are Enriched in the Compact SAN and Transitional Cells of the Mouse Heart.



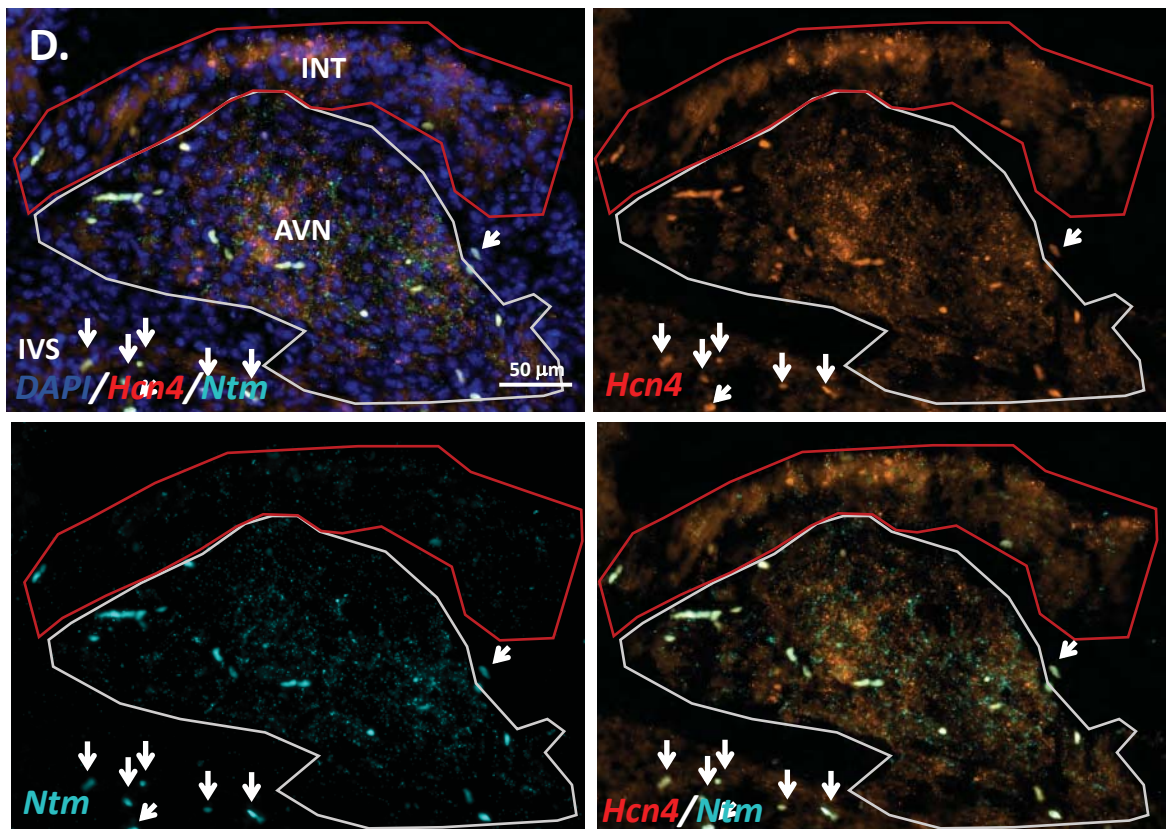
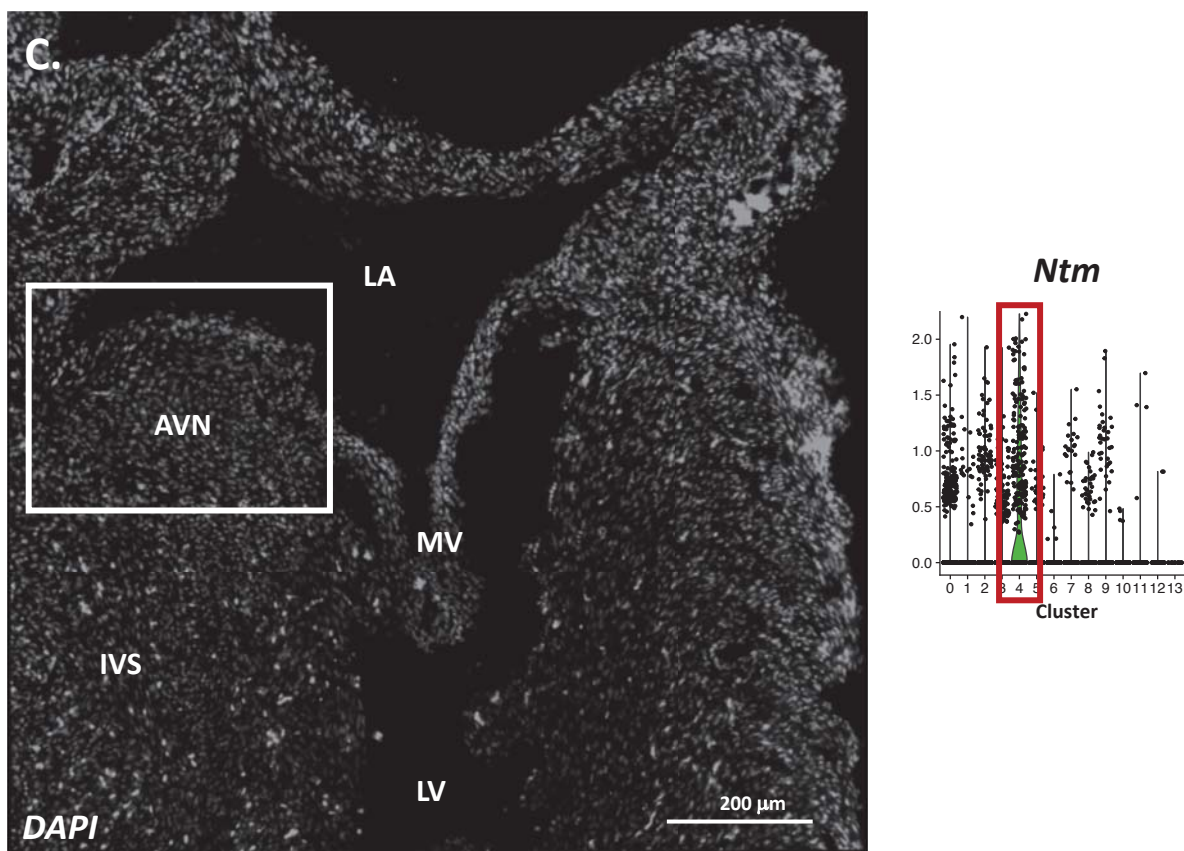
Online Figure VI. Expression of *Igfbp5*, *Cpne5*, *Rgs6* and *Ntm* Within cSAN and Transitional Cell Subclusters of Cluster 9.



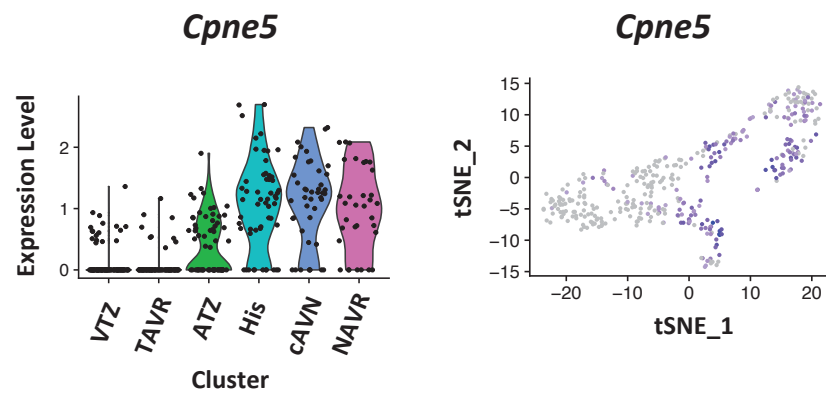
Online Figure VII. Analysis of *Hcn4*⁺ Cells in Zone I Reveal Compact SAN Subtypes Consistent with Head and Tail Regions.



Online Figure VIII. *Igfbp5*, *Rgs6* and *Ntm* are Enriched in the Murine AVN.

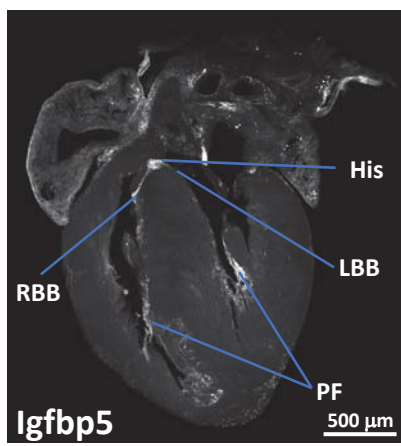


Online Figure VIII...continued. *Igfbp5*, *Rgs6* and *Ntm* are Enriched in the Murine AVN.

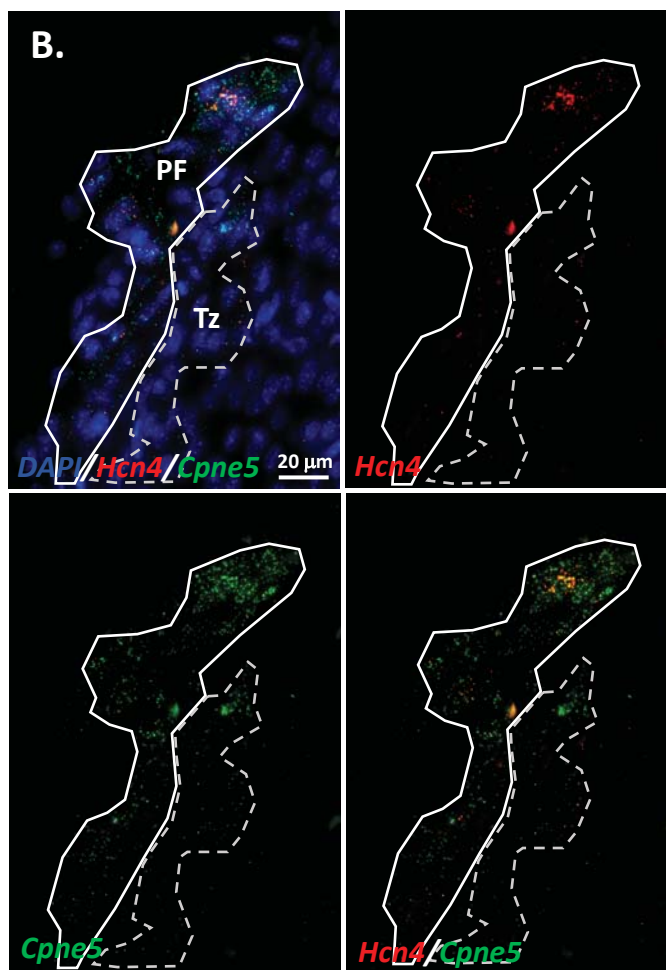


Online Figure IX. *Cpne5* Expression in Cluster 4 Cell Subtypes.

A.



B.

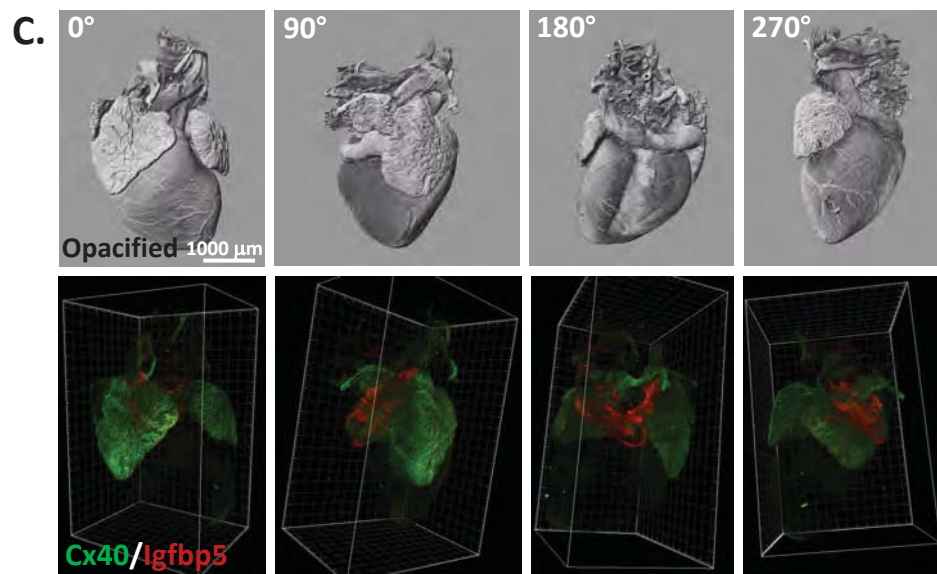
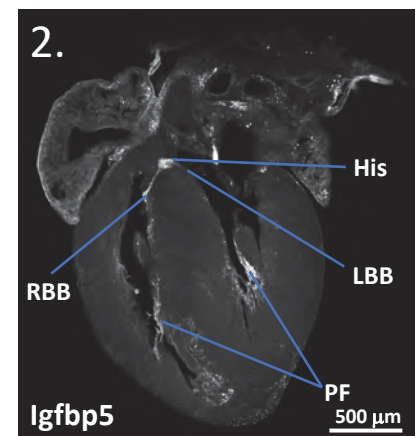
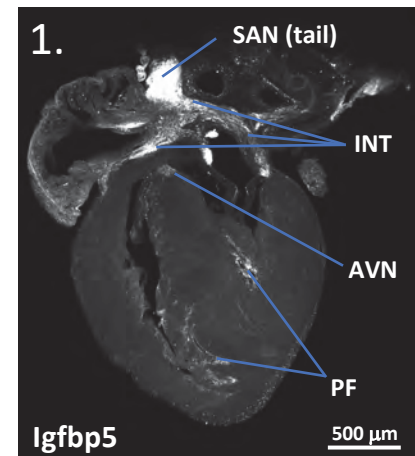


Online Figure X. *Igfbp5* and *Cpne5* Are Expressed in the Ventricular Conduction System.

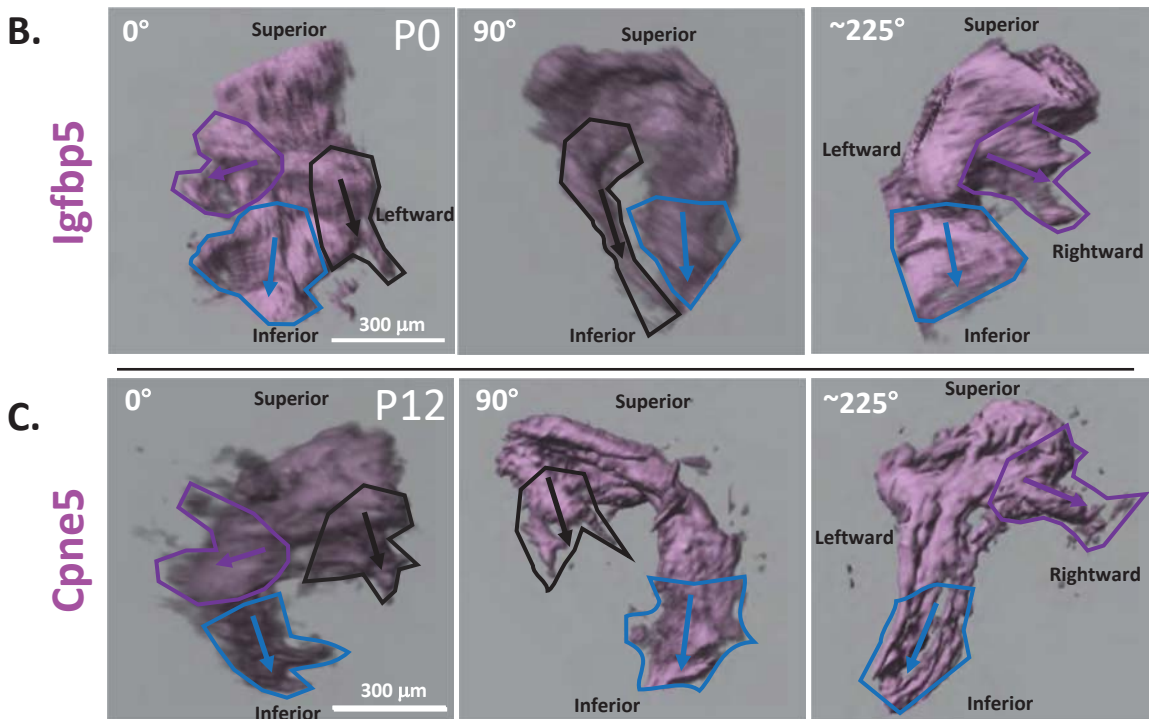
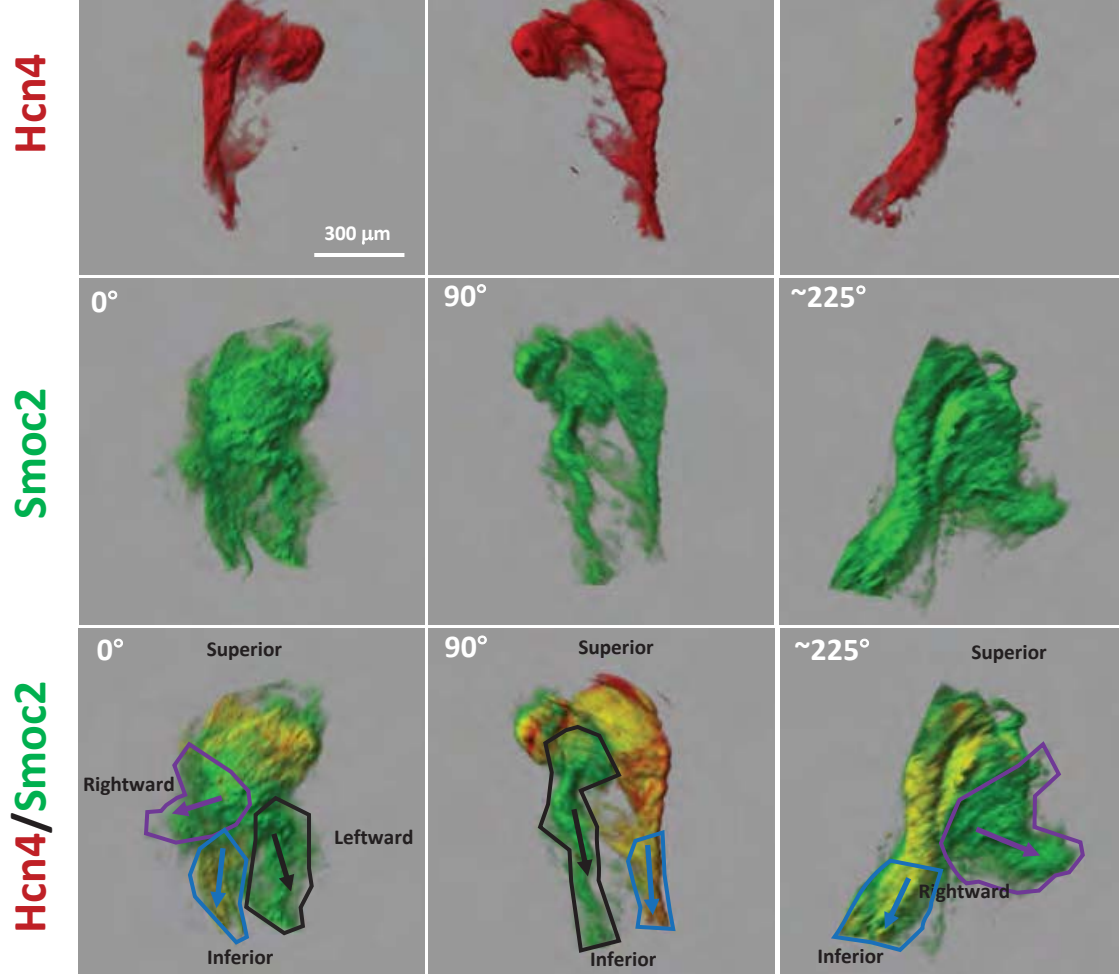
Gene: <i>Igfbp5</i>		
Cell Type	Avg Log FC	p value (adj)
SAN (Cluster 9 vs. all Zone I)	2.12	2.63E-126
AVN (Cluster 4 vs. all Zone II)	1.19	1.49E-120
PF (Cluster 13 vs. all Zone III)	0.96	1.11E-100



2D Z-projections



Online Figure XI. *Igfbp5* is Enriched Within the Entire Cardiac Conduction System.



Online Figure XII. Optical Clearing and 3D Volumetric Analyses Illustrate Transitional Cell Populations Exiting the SAN.